

# Immunohistochemical Analysis of Transcription Factors and Markers of Epithelial–Mesenchymal Transition (EMT) in Human Tumors

JASAMIN GHULAM<sup>1</sup>, CHRISTINE STUERKEN<sup>1</sup>, DANIEL WICKLEIN<sup>1</sup>,  
RALPH PRIES<sup>2</sup>, BARBARA WOLLENBERG<sup>2</sup> and UDO SCHUMACHER<sup>1</sup>

<sup>1</sup>*Institute of Anatomy and Experimental Morphology, University Cancer Center Hamburg,  
University Medical Center Hamburg-Eppendorf, Hamburg, Germany;*

<sup>2</sup>*Department of Otorhinolaryngology, University of Lübeck, Lübeck, Germany*

**Abstract.** *Background/Aim: Epithelial–mesenchymal transition (EMT) is a key multi-step process which enables cancer cells to detach from the epithelial primary tumor mass and allows them to metastasize to distant organs. We immunohistochemically analyzed the expression of the transcription factors (TWIST-1, SLUG, ZEB1, ZEB2) and components of the extracellular matrix (laminin-5, fibronectin) which influence the EMT. Materials and Methods: Primary human breast (MDA-MB-231), colon (HT29, HCT116), ovarian (SKOV3, OVCAR3) and head and neck squamous cell carcinoma cell lines (UTSCC2, UTSCC24A) grown as xenografts were immunohistochemically analyzed in vitro and in vivo. Results: A high SLUG expression was observed in every cancer entity both in vitro and in vivo. ZEB1 and ZEB2 showed a high in vivo expression especially in SKOV3 and in in vitro grown MDA-MB-231 cells. Conclusion: SLUG expression showed the highest expression in all cancer entities investigated. Hence, it presumably represents the master regulator of EMT in these metastatic tumor entities.*

Epithelial–mesenchymal transition (EMT) is a cascade of cellular regulatory events playing an essential role in the invasiveness and metastasis formation of solid neoplasms. During this process cancer cells lose their epithelial properties such as cell-to-cell and cell-to-matrix contacts and acquire mesenchymal characteristics which enable them to migrate

through the extracellular matrix. EMT is associated with a considerable alteration in gene expression pattern which includes an up-regulation of mesenchymal proteins (*e.g.* vimentin, N-cadherin, matrix metalloproteinases and members of the Wnt pathway family) and concomitant decrease in the expression of proteins typically expressed in epithelia (*e.g.* E-cadherin, actin and cytokeratins). The result of this process is a rearrangement of the cytoskeleton and the acquisition of a migratory phenotype. Therefore, EMT induces invasion of surrounding tissues, which is a necessary step for metastasis formation in malignant tumors. EMT itself is regulated by a number of transcription factors including SLUG, TWIST, ZEB1 and ZEB2 (zinc-finger E-box binding homeobox 1 and 2). SLUG, also known as SNAI2 acts as a transcriptional repressor, binds to E-box motifs and causes desmosome dissociation (1). It furthermore acts as a repressor for example, of E-cadherin transcription in breast cancer cells causing mesenchymal-specific proteins to be expressed resulting in induction of EMT. SLUG can also induce breast cancer by activating a silencer that negatively regulates the function of the *BRCA2* gene promoter, which itself acts as a tumor suppressor gene (2). TWIST is expressed in cells of many different tissues including bone marrow, lymph nodes, neurons, muscle cells and in secretory epithelia of, for example, pancreas and thyroid gland. TWIST induces EMT by activating gene expression of the miRNA10b, which positively regulates cell migration and invasion in breast cancer (3).

ZEB1 and ZEB2 can interact directly with promoter sequences of cellular DNA and repress the expression of epithelial-specific genes such as E-cadherin and thus facilitate the induction of EMT (4–6). These specific epithelial genes are regulated by the miR-200 family microRNAs, which influence gene expression networks by repressing target messenger RNAs (mRNA) specific for epithelia (7).

Hence, ZEB1 and 2 are known as mesenchymal markers which have been investigated in many tumor entities, including

*Correspondence to:* Jasamin Ghulam, Institute of Anatomy and Experimental Morphology, University Cancer Center Hamburg, University Medical Center Hamburg-Eppendorf, Martinistraße 52, 20246 Hamburg, Germany. Tel: +49 0741052586, Fax: +49 0741055427, e-mail: Jasamin@gmx.de

*Key Words:* Epithelial–mesenchymal transition, metastasis, SLUG, transcription factor, TWIST-1, ZEB1, ZEB2, xenograft tumors.

Table I. Origin and characteristics of tumor cell lines used in this study.

Cell line	Origin
Breast	
MDA-MB-231	Breast cancer is the most frequent gynecological tumor. The cell line MDA-MB-231 we have focused on in this study is an aggressive type of breast cancer
Colon	
HCT116 HT29	Colon cancer is one of the most malignant diseases and takes the second place in the ranking of the most common forms of cancer in the Western world. The cell lines HT29 and HCT116 used in the study have both epithelial characteristics
Ovarian	
Skov3 Ovarc3	Ovarian cancer is one of the most aggressive gynecological tumors with a severe prognosis. It still causes death in many cases due to the lack of effective early detection methods. The only validated marker in current use is CA125
HNSCC	
UTSCC2 UTSCC24A	Head and neck squamous cell cancer is one of the most common malignant cancers worldwide. The cell lines we have chosen are the ones with the highest rates of lung metastases.

colon cancer, ovarian cancer and breast cancer (8-10). S100A4 is a member of the S100-family of proteins and can, like SLUG and TWIST, be localized in the cytoplasm and/or the nucleus. It is involved in the regulation of a number of cellular processes such as cell cycle progression and differentiation (11). Phenotypically, EMT is characterized by the induction of metalloproteinases which degrade the basement membrane (BM) and the expression of laminin-5 and its receptors in the BM resulting in an invasive phenotype (12, 13).

The aim of this study was to investigate the expression of different EMT markers in parallel in human cancers xenografted into immunodeficient mice in order to determine whether there is a correlation between the expression of the different transcription factors or not. In addition, we investigated the expression of extracellular matrix proteins that undergo turnover during EMT or which are typically expressed in the mesenchymal (vimentin) or epithelial (cytokeratin, EpCAM) differentiation state. Tumors of the following entities were investigated: colon adenocarcinoma, head and neck squamous cell cancer (HNSCC) breast and ovarian cancer (Table I). With the exception of the UTSCC2 cell line, which was not metastatic, all other cell lines had been proven to be metastatic in previous xenograft experiments, from which the tissue blocks were retrieved.

## Materials and Methods

**Cell and tissue preparation.** Tissue blocks, fixed in formaldehyde and paraffin-embedded, were drawn from the archives of the Institute of Anatomy and Experimental Morphology. All cell lines were systemically or in the case of ovarian cancer intraperitoneally metastatic upon transplantation into immunodeficient mice. They belong to four different tumor entities including colon cancer [HT29, HCT116 (14)], head and neck squamous cell carcinoma (HNSCC; UTSCC2 and 24A), breast cancer [MDA-MB-231 (15)] and ovarian cancer [SKOV3, OVCAR3 (16)] (Table I).

Primary tumors growing subcutaneously and spontaneous pulmonary metastases from SCID mice as well as tumor cells grown *in vitro* were analyzed. The cells grown *in vitro* were harvested by a cell scraper and fixed in neutral buffered formalin. Thereafter, they were centrifuged and embedded in 4% DifcoAgar Noble. These cell pellets were processed in the same way as solid tissue. In case of ovarian cancer, primary tumor nodules grown intraperitoneally, were used. Four µm thick sections were cut, rehydrated *via* xylene and graded ethanol series, and pretreated according to the individual antibody used, and different antigen retrieval methods were applied dependent on the antibody used. Pretreatment included heat (from 4 min with 100°C in a microwave, 10 to 20 min in a steamer (DakoCytomationPascal; DC1517, CA, USA) or overnight in a water bath from 80-100°C], or enzyme-mediated with a fast enzyme for 5 min (ZytomedSystems, 15 ml ready-to-use, REF ZUC059-015, LOT M813; Diagnostic Biosystems, CA, USA) (Tables II and III). After a rinse in Tris- buffered saline with Tween added (2 ml of 20% Tween, TBS-T, pH 7.6; two times for 5 min each) and once in TBS for 5 min (pH 7.6) sections were incubated with the primary antibody for 30 min (if Dako REAL™ Detection System, K5005 was used) or alternatively for one h at room temperature with the respective control antibodies in Dako Antibody Diluent, Background Reducing (S3022). Primary antibodies were antibodies against SLUG, TWIST, ZEB1 and ZEB2, S100A4, Fibronectin, Laminin-5, Pan-Cytokeratin, Vimentin, ICAM-1 and EpCAM. Afterwards, sections were rinsed in TBS-T again and incubated with secondary antibody Dako polyclonal biotinylated swine-anti-rabbit immunoglobulins (0.51 g/l) in a 1:200 dilution in TBS for 30 min at room temperature. Slides were again rinsed in TBS-T. The antibody binding sites were visualized with the Avidin-Alkaline Phosphatase-Complex (ABC, Vectastain, ABC Kit, AK-5000; Vector Laboratories Inc., Burlingame, CA, USA) and incubated for 30 min at room temperature with ABC reagent (Tables II and III). After rinsing in Tris-buffered saline with Tween added (2 ml of 20% Tween, TBS-T, pH 7.6; twice for 5 min each), and once in TBS (pH 7.6) for 5 min, sections were incubated with the primary antibody for 30 min (if Dako REAL™ Detection System, K5005 was used), or alternatively for one h at room temperature with the respective control antibodies in Dako Antibody Diluent, Background Reducing (S3022). Primary antibodies were antibodies against SLUG, TWIST,

Table II. Immunohistochemical methods used in this study– transcription factors.

Primary antibody		Pretreatment	Concentration	Negative control	Secondary antibody	Detection system
SLUG (LifeSpan Bioscience LS-B3449)	Snail-2	Slides covered with S1699 (Target Retrieval Solution, Dako) and steamed at 121°C for 20 min	1 mg/ml (1:100)	Rabbit negative control (1:1900, Dako X0903,	Dako REAL™ detection System (K5005) 19 g/l)	Chromogen red
S100A4 (Dako, A1554)	S100 Calcium-Binding ProteinA 4	Slides buffered in citrate and put into water quench at 60°C over night	1 g/l (1:10)	Rabbit negative control (1:200, Dako X0903, 19 g/l)	Swine anti rabbit (1:200, Dako E0353, 0.51 g/l)	ABC-AP and permanent red
TWIST (Abcam, ab50581)	Twist family bHLH Transcription-factor	Slides covered with S1699 (Target Retrieval Solution, Dako) and steamed at 121°C for 20 min	1.1 mg/ml (1:200)	Rabbit negative control (1:1900, Dako X0903, 19 g/l)	Swine anti rabbit (1:200, Dako E0353, 0.51 g/l)	ABC-AP and permanent red
ZEB1 (Sigma, HPA002 7524)	Zink Finger E-Box-Binding Homeo-box1	Slides covered with S1699 (Target Retrieval Solution)	0.2 mg/ml (1:100)	Rabbit negative control (1:10000, DakoX0903, 19 g/l)	Swine anti rabbit (1:200, Dako E0353, 0.51 g/l)	ABC-AP and permanent red
ZEB2 (Sigma, HPA00 3456)	Zink Finger E-Box-Binding Homeo-box2	Dako and steamed at 121°C for 10 min	0.1 mg/ml (1:100)	Rabbit negative control (1:19000, Dako X0903, 19 g/l)	Dako REAL™ Detection System (K5005)	Chromogen red

Table III. Immunohistochemical methods used in this study– matrix proteins.

Primary antibody		Pretreatment	Concentration	Negative control	Secondary antibody	Detection system
ICAM-1 (Santa Cruz, sc-8439)	Inter-cellular Adhesion molecule (CD54)	2×4 min at 100°C in the microwave in S1699 (Target Retrieval Solution, Dako)	200 µg/ml (1:500)	Mouse IgG2a (1:250, Dako X0943, 100 mg/l)	Dako REAL™ detection system (K5005)	Chromogen red
EpCAM (Dako, M3525)	Epithelial cell adhesion molecule (MOC-31)	Proteinase (40 mg/100 ml) at 37°C in the water quench for 10 min	43 mg/l (1:35)	Mouse IgG1 (1:59, Dako X0931, 100 mg/l)	Goat anti mouse (1:200, Dako E0433, 0.77 g/l)	ABC-AP and permanent red
Fibronectin (Dako, A0249)	FN1	2×4 min at 100°C in the microwave in S1699 (Target Retrieval Solution, Dako)	4.9 g/l (1:8000)	Rabbit negative control (1:31200, DakoX0903, 19 g/l)	Swine anti rabbit (1:200, Dako E0353, 0.51 g/l)	ABC-AP and permanent red
Laminin-5 (Abcam, ab78286)	Lam-5	Fast enzyme for 5 min	1 mg/ml (1:200)	Mouse IgG1 (1:20, Dako X0931, 100 mg/l)	Goat anti mouse (1:200, Dako E0433, 0.77g/l)	ABC-AP and permanent red
PanCytokeratin (Dako, M3515)		Cooked for 1min in the microwave in S1699 (Target Retrieval Solution, Dako) and then at 95°C in the water quench for another 20 min	1 mg/ml (1:10)	Mouse IgG1 (1:8, Dako X0931, 100 mg/l)	Goat anti mouse (1:200, Dako E0433, 0.77g/l)	ABC AP and permanent red
Vimentin (Dako, M7020)		S1699 (Target Retrieval Solution, Dako) in the water quench over night at 85°C	62-64 mg/l (1:150)	Mouse IgG2a (1:375, Dako X0943, 100 mg/l)	Goat anti mouse (1:200, Dako E0433, 0.77 g/l)	ABC-POX and staining with DAB

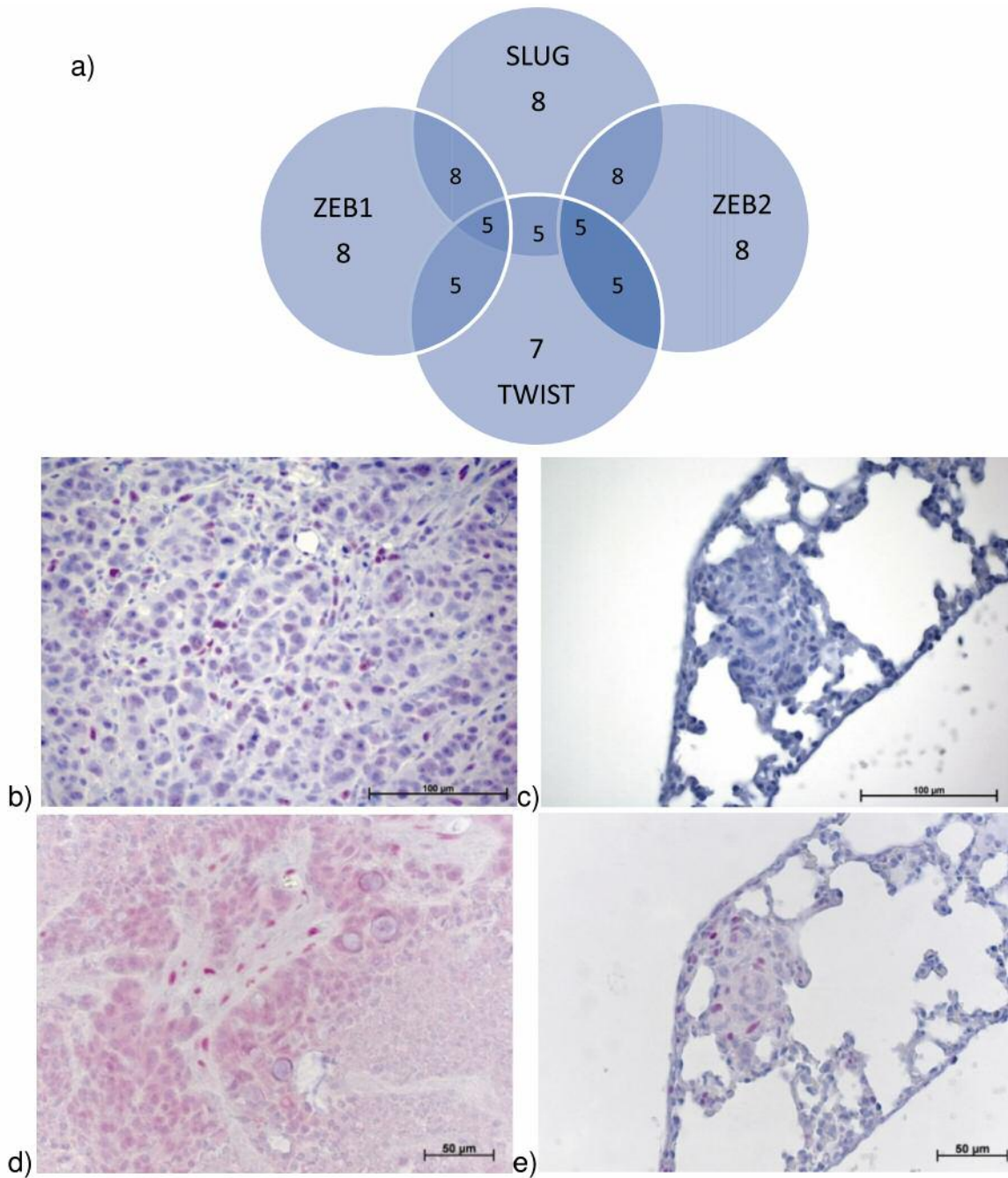


Figure 1. Transcription factor expression and immunohistochemical staining in HCT116 and HT29 of colon cancer: (a) correlation of SLUG, TWIST, ZEB1 and ZEB2 in primary tumor of colon cancer (includes cell lines HT29 and HCT116; numbers show amount of staining and overlap between the transcription factors in vivo (b) expression of ZEB1 in HT29 in vivo, (c) expression of ZEB1 in HT29 in pulmonary metastasis, (d) expression of ZEB2 in HT29 in vivo, (e) expression of ZEB2 in HT29 in pulmonary metastasis.

ZEB1 and ZEB2, S100A4, fibronectin, laminin-5, pan-cytokeratin, vimentin, ICAM-1 and EpCAM. Afterwards, the sections were rinsed in TBS-T again and incubated with secondary antibody Dako polyclonal biotinylated swine-anti-rabbit immunoglobulins (0.51 g/l) in a 1:200 dilution in TBS for 30 min at room

temperature. Slides were again rinsed in TBS-T. The antibody binding sites were visualized using the Avidin-Alkaline Phosphatase-Complex (ABC, Vectastain, ABC Kit, AK-5000; Vector Laboratories Inc., Burlingame, CA, USA) and incubated for 30 min at room temperature with ABC reagent (Tables II and III). After

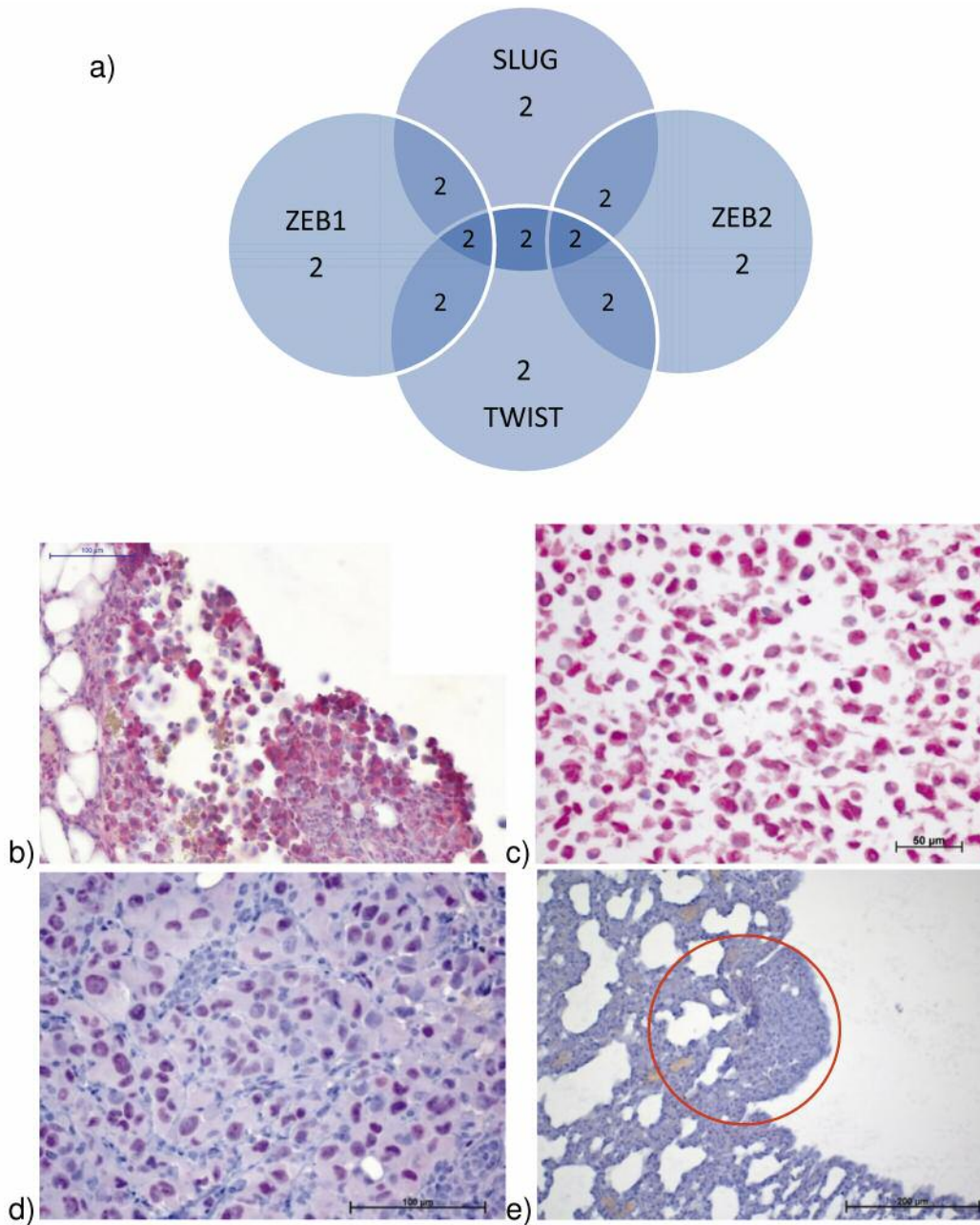


Figure 2. Transcription factor expression and immunohistochemical staining in MDA MB231 of breast cancer: (a) correlation of SLUG, TWIST, ZEB1 and ZEB2 in primary tumor of breast cancer with cell line MDA-MB-231; numbers show the amount of staining and overlap between transcription factors in vivo, (b) expression of SLUG in MDA-MB-231 in vivo (scale bar shows 100 μm), (c) expression of SLUG in vitro (scale bar shows 200 μm), (d) expression of ZEB1 in vivo, (e) expression of ZEB1 in pulmonary metastasis.

three rinses in TBS-T, slides were incubated with Dako Liquid Permanent Red Reagent for up to 30 min. The sections were washed under running water for 5 min; afterwards, they were dipped for one to two min in distilled water and then counterstained with hemalum, dehydrated in a series of graded ethanol, immersed in xylene and mounted with Eukitt (mounting medium for microscopy, O. Kindler

GmbH, Freiburg, Germany). Images were taken on a Zeiss Axiophot microscope equipped with a Zeiss MRc2 camera (Carl Zeiss, Göttingen, Germany). The immunoreactivity of the different antibodies was scored into four different staining intensity levels: negative 0), very weak staining 1), moderate positivity 2), and very intensive 3) immunoreactivity.

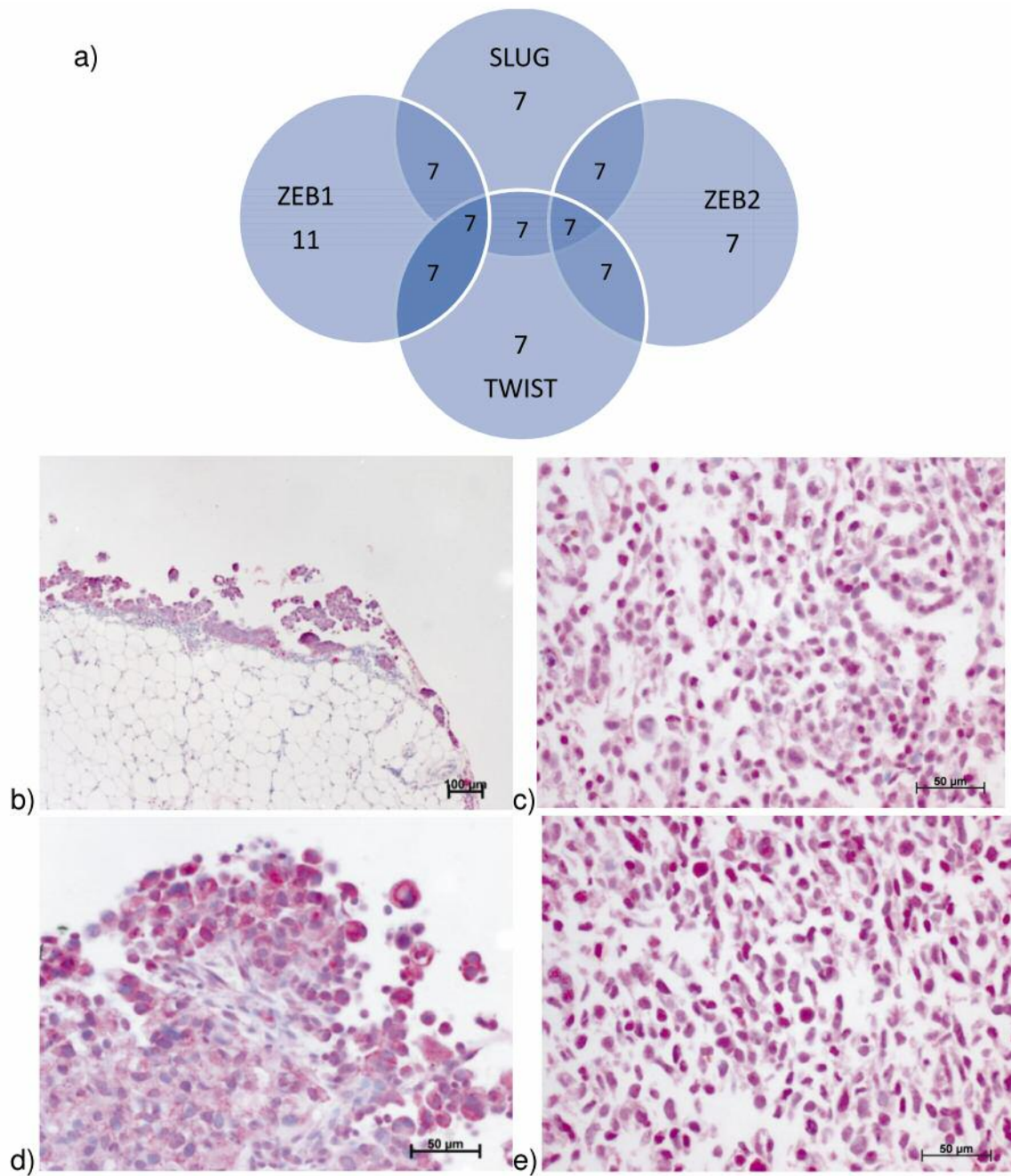


Figure 3. Transcription factor expression and immunohistochemical staining in SKOV3 and OVCAR3 of ovarian cancer: (a) correlation of SLUG, TWIST, ZEB1 and ZEB2 in primary tumor of ovarian cancer (includes cell lines SKOV3 and OVCAR3); numbers show amount of staining and overlap between transcription factors in vivo, (b) expression of SLUG in OVCAR3 in vivo, (c) expression of SLUG in OVCAR3 in vitro, (d) expression of SLUG in SKOV3 in vivo, (e) expression of SLUG in SKOV3 in vitro (scale bar shows 50 μm).

## Results

Expression of transcription factors and EMT markers in colon cancer. The expression of SLUG showed the same results in

HCT116 and HT29 cells: cells grown *in vitro* and embedded in cell pellets were intensively labeled, and showed an especially high immunoreactivity in their nuclei. Only in a few *in vitro* grown HCT116 and HT29 cells SLUG immunoreactivity was

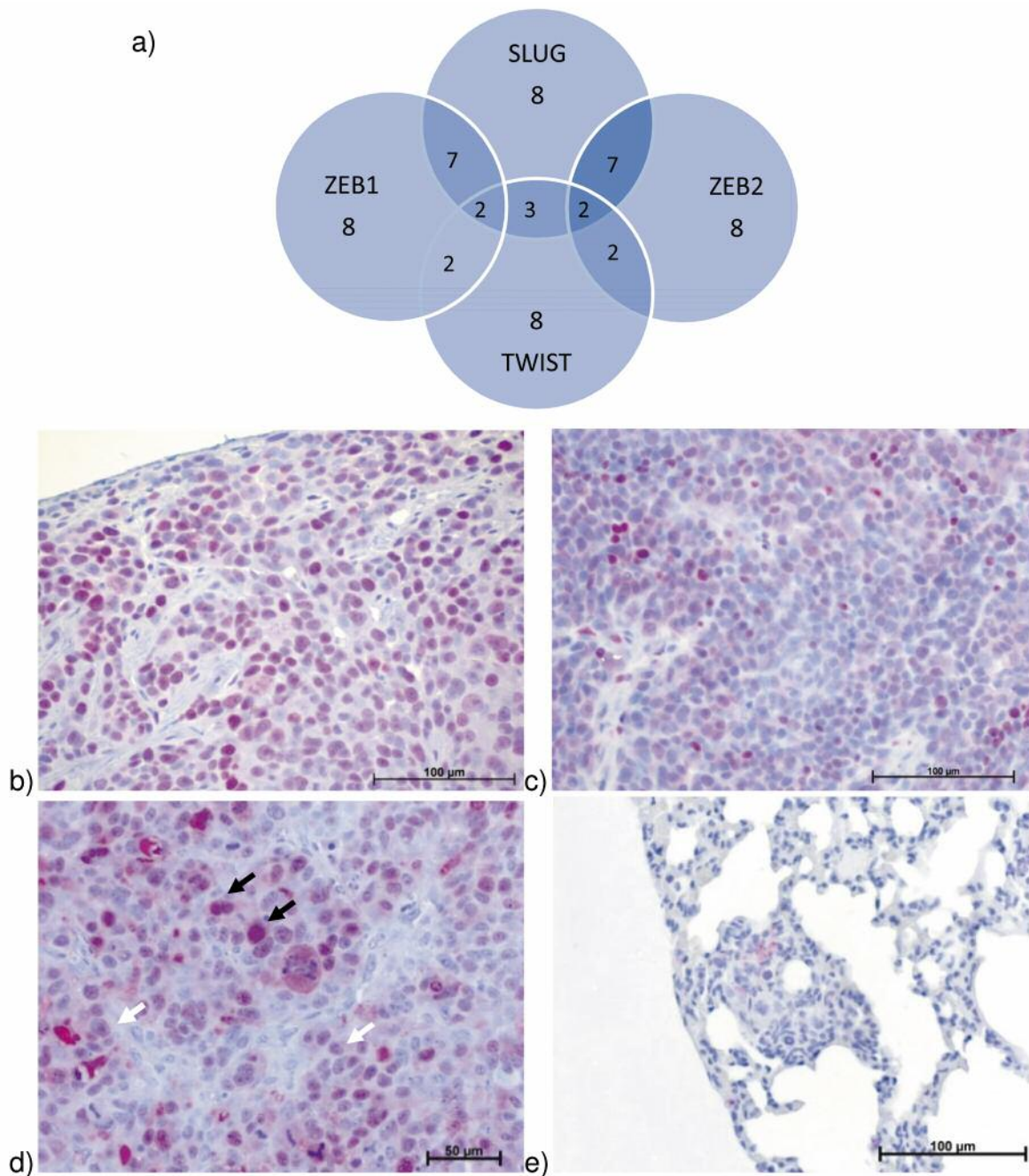


Figure 4. Transcription factor expression and immunohistochemical staining in UTSCC2 and UTSCC24A of HNSCC: (a) correlation of SLUG, TWIST, ZEB1 and ZEB2 in primary tumor of HNSCC (includes UTSCC2 and UTSCC24A); numbers show the amount of staining and overlap between transcription factors *in vivo*; note that only three had positive staining for TWIST, (b) moderate expression of ZEB1 in UTSCC2 *in vivo*, (c) low expression of ZEB2 in UTSCC2 *in vivo* (b+c: same pattern in UTSCC24A, image are not shown here), (d) expression of S100A4 in UTSCC24A and corresponding pulmonary metastases, (e) large metastasis (white arrows show nuclear expression and black arrows cytoplasmic expression of S100A4).

also localized in the cytoplasm. Particularly in cells of the tumor-host interface, high SLUG expression was noted in the nucleus. SLUG expression in the nuclei of HCT116 and HT29 cells of spontaneous lung metastases was not observed;

however, it was just above the detection level in the cytoplasm of some of the metastatic cells (Figure 1).

TWIST immunoreactivity in the nucleus was low both *in vivo* in primary tumors and in spontaneous lung metastases,

as well as in *in vitro* grown HT29 and HCT116 cells. ZEB1 expression was absent in HCT116 and HT29 primary tumor cells and their lung metastases and also in the cells grown *in vitro*. However, moderate expression was noted in stromal cells of the primary tumors in both cell lines. While ZEB2 expression was also absent in HCT116 and HT29 cancer cells of the primary tumors, the nuclei of the stromal cells showed a very high ZEB2 expression. Remarkably, the ZEB2-positive stroma cells surrounded the local venous vessels within the primary tumor mass in both cell lines. Correspondingly, cancer cells in the spontaneous lung metastases contained a few individual cancer cells whose nuclei were highly ZEB2 immunoreactive (Figure 2). S100A4 showed moderate to high cytoplasmic immunoreactivity in a few individual HT29 and HCT116 cells of primary tumors and their metastases. *In vitro* grown cells of both cell lines in the cell pellets were S100A4 negative. Fibronectin was highly expressed in the ECM of the tumor stroma and in the BM of the blood vessels in both cell lines. In contrast, HT29 and HCT116 cells grown *in vitro* showed a high expression of both proteins in their cytoplasm. The pulmonary metastases also had a few cells that were positive. Laminin-5 was expressed in the matrix at the tumor-host interface, especially nearby the vessels. Spontaneous lung metastases showed a high expression level of laminin-5 in the extracellular matrix, while *in vitro* grown cells showed a low expression level of both proteins in their cytoplasm. HT29 and HCT116 cells grown *in vitro* highly expressed pan-cytokeratin at the tumor-host interface. In contrast, HT29 and HCT116 cancer cells in the center of the primary tumors were generally negative, while a low to moderate staining of some cells at the tumor-host interface could be observed. Metastases were also negative. Vimentin expression was not observed in both colon cancer cell lines *in vivo* and *in vitro*. EpCAM showed a very high cell membrane expression in HT29 and HCT116 cancer cells of primary tumors *in vitro* and *in vivo* and a low to moderate cell membrane expression in cancer cells of lung metastases. Cell pellets of HCT116 cells were only faintly stained for ICAM-1; HT29 cells grown *in vitro* were stained highly positive for ICAM-1, while *in vivo* cells and metastases were negative.

*Expression of transcription factors and EMT markers in breast cancer.* MDA-MB-231 cells showed a very high nuclear and cytoplasmic SLUG expression *in vitro*, which was also noted in primary tumor cells and especially in cells of the tumor-host interface. Metastatic cells were characterized by a high nuclear SLUG expression. TWIST expression *in vitro* was cytoplasmic, but compared to SLUG, just at a moderate expression level. Primary tumors expressed TWIST in the same way as SLUG: cytoplasmic expression in cancer cells of the tumor-host interface, while no TWIST-stained metastases were noted. ZEB1 cytoplasmic expression was low to absent in *in vitro* grown cells. Only Fra2-overexpressing (clone 8)

primary MDA-MB-231 tumor cells expressed ZEB1 abundantly in the cytoplasm, while metastases were ZEB1 negative. ZEB2 expression in cancer cells of primary tumors was high in the nuclei as well as in the cytoplasm. Metastases and cells grown *in vitro* were stained just faintly in the cytoplasm. S100A4 expression *in vitro* showed a high expression in the cytoplasm of breast cancer cells. Just a few cells at the tumor-host interface of the primary tumor expressed S100A4 at a high level, located in both cytoplasm and nucleus. Fibronectin was not expressed in cells grown *in vivo* or *in vitro* and in metastases. It was, however, expressed in the connective tissue septa of the tumors and in the connective tissue stroma surrounding the tumor. Cells grown *in vitro* showed a high laminin-5 expression in the cytoplasm. Cancer cells of the primary tumors, especially those at the tumor-host interface, also showed a high cytoplasmic expression. Pan-cytokeratin was expressed in most cells grown *in vitro*. It was detected at the margin of the cells, such as in HT29 and SKOV3 cells. A low intracytoplasmic vimentin expression was noted in cells grown *in vitro*. In contrast, there was a high cytoplasmic expression in cancer cells grown as primary tumors, in some fibroblasts and in some mononuclear cells. *In vitro* expression of ICAM-1 was located at the cell membrane of nearly all cancer cells grown *in vitro*. While the majority of cancer cells were ICAM-1 negative, cancer cells located at the tumor-host interface of the primary tumor showed a high membrane expression. MDA-MB-231 cells were always EpCAM negative.

*Expression of transcription factors and EMT markers in ovarian cancer.* The ovarian cancer SKOV3 and OVCAR3 cells showed the same pattern of SLUG expression: the vast majority of ovarian cancer cells grown *in vitro* were intensively intracytoplasmically labeled by the anti-SLUG antibody (Figure 3). Cancer cells of primary tumors which expressed SLUG intracytoplasmically at a high level were solely detected at the tumor-host interface. Cancer cells of intraperitoneal (ip) metastases showed the same pattern as in primary tumors. Pulmonary metastases were not detected. TWIST expression *in vitro*, *in vivo* and in metastases was high in SKOV3 cells. *In vitro* cells expressed TWIST in the nucleus as well as in the cytoplasm. Cells at the tumor-host interface of primary tumors and intraperitoneal metastases expressed TWIST only in the nucleus. The cells were located in the stroma beneath the peritoneum, or had just attached to it. OVCAR3 cells showed a weak nuclear and cytoplasmic expression of TWIST in cells grown *in vitro*. Cells of the primary tumors at the tumor-host interface were intensively stained in both cellular compartments by the anti-TWIST antibody. OVCAR3 cells of the intraperitoneal metastases showed the same staining pattern as in the primary tumors. High cytoplasmic and nuclear expression of TWIST was noted in cells located at the tumor-host interface. ZEB1 expression

in SKOV3 cells was high in all tissues investigated. Cells grown *in vitro* showed a high cytoplasmic ZEB1 expression of almost all cells. Cancer cells of the primary tumor showed a cytoplasmic and nuclear staining of cancer cells spread all over the tumor, but especially pronounced expression was observed in cells located at the tumor-host interface. Cancer cells of the intraperitoneal metastases also expressed ZEB1 at a high intensity, and also both in the nucleus and in the cytoplasm. ZEB1 positive cells were mainly located in the stroma and were closely related to blood vessels. Pulmonary metastases were not detected. In contrast, OVCAR3 cells showed a weak ZEB1 expression *in vitro* and *in vivo*.

No ZEB2 expression was noted in SKOV3 and OVCAR3 cells grown *in vitro*. In contrast, ZEB2 expression was highly expressed in SKOV3 cells grown *in vivo* and in metastases, while it was weak in OVCAR3 grown *in vivo* and in metastases. ZEB2 expression was both nuclear and cytoplasmic. S100A4 expression showed a low cytoplasmic intensity *in vitro* in both cell lines, and a high cytoplasmic intensity was noted in primary tumor cells and in intraperitoneal metastatic cells. *In vivo* S100A4 positive SKOV3 cancer cells were located around the peritoneum, fat cells and in the stroma. S100A4 OVCAR3 cells were present ubiquitously within the tumor mass. Fibronectin expression showed the same pattern in SKOV3 and OVCAR3 cells. Cells grown *in vivo* showed no fibronectin expression. Fibronectin deposits could be found in ECM and along the blood vessels in a moderate intensity in SKOV3 and OVCAR3 primary tumors. Fibronectin was strongly expressed in the BM in the ECM below the mesothelium. Laminin-5 showed an opposite expression pattern between SKOV3 and OVCAR3 cells. While SKOV3 cells showed a weak cytoplasmic expression *in vitro*, OVCAR3 cells showed a strong cytoplasmic expression. SKOV3 primary tumor cells and cells of intraperitoneal metastases located at the tumor-host interface showed a high laminin-5 expression. Cells of primary tumors and intraperitoneal metastases were negative. Pan-cytokeratin expression was high and was located at the membrane of cells in SKOV3 and OVCAR3 cells. It was mainly the cells in the center of the tumor, and not those at the tumor-host interface, that were positive for pan-cytokeratin. The pan-cytokeratin-positive cancer cells were often located around blood vessels. This behavior could be found in primary tumors as well as in intraperitoneal metastases. Vimentin was negative in all SKOV3 and OVCAR3 cells. ICAM-1 showed a similar expression pattern in SKOV3 and OVCAR3 cells. Primary tumor cells and cells of the intraperitoneal metastases located at the tumor-host interface highly expressed ICAM-1 in their cell membranes. *In vitro*, only few SKOV3 cells were faintly ICAM-1 positive, while the majority of OVCAR3 cells were intensively stained for ICAM-1. EpCAM expression was negative in SKOV3 cells in all tissues. In contrast, OVCAR3

cells showed a weak membranous staining of cells at the tumor-host interface. In cells of the intraperitoneal metastases, EpCAM was expressed at a moderate to high level.

*Expression of transcription factors and EMT markers in head and neck squamous cell cancer.* High SLUG expression was detected mainly in the nucleus of both head and neck squamous cell cancer non-metastatic UTSCC2 cells and metastatic UTSCC24A cells. In addition to the cancer cells, stromal cells were mainly stained in the nucleus. Cells grown *in vitro*, and cells grown as primary tumors, as well as cancer cells of the pulmonary metastases, showed the same staining pattern. TWIST expression in UTSCC2 and UTSCC24A cells showed a similar staining pattern. Cells grown *in vitro* moderately expressed TWIST in the nucleus, while nuclear expression in cancer cells of the primary tumor was low to moderate, with only a few cells at the tumor-host interface being stained. UTSCC2 cells showed an absent or just a low expression in primary tumors and UTSCC24A cells showed a moderate expression of TWIST in the same tissue. Metastases of UTSCC24A positive cells of xenografted mice were TWIST negative. ZEB1 expression of *in vitro* grown UTSCC2 cells showed a moderate cytoplasmic expression in many cells. ZEB1 expression *in vivo* was predominantly seen in tumor cells at the tumor-host interface, where they expressed ZEB1 at a moderate level, and mainly in the cytoplasm. Metastases were not detected. In contrast, UTSCC24A showed a different expression pattern of ZEB1. Just a few *in vivo* cells expressed it in a very low cytoplasmic intensity. Cancer cells of primary tumors located at the tumor-host interface also expressed ZEB1 with a low nuclear intensity. However, expression of ZEB1 was higher in the cytoplasm of stromal cells. Pulmonary metastases were negative for ZEB1 expression. UTSCC2 cells grown *in vitro* expressed ZEB2 at a very low level intra-cytoplasmically, while cancer cells in primary tumors expressed it in the nucleus. ZEB2 expression could not be detected in metastases. ZEB2 expression in UTSCC24A cells showed a similar expression pattern. UTSCC24A cells grown *in vitro* showed no ZEB2 expression. Only a few cancer cells from primary UTSCC24A tumors were stained for ZEB2 in their nuclei. A more intensive cytoplasmic ZEB2 immunoreactivity was noted in the cytoplasm of stromal fibroblasts. Expression in pulmonary metastases was weak in stromal cells, while UTSCC24A cancer cells were negative. The expression of S100A4 in HNSCC was different in both cell lines. While S100A4 expression in UTSCC2 cells was low in the cytoplasm of primary tumor cells, its expression was high in cells grown *in vitro*. *In vitro* grown UTSCC24A cells, as well as cells in primary tumors, showed a high cytoplasmic expression of S100A4. S100A4 positive cancer cells were located mainly at the tumor-host interface. Pulmonary metastases could not be detected in UTSCC2, but were found in UTSCC24A cells;

they showed just a low cytoplasmic staining. Cells of both cell lines grown *in vitro* did not express fibronectin. *In vivo*, fibronectin was highly expressed in the extracellular matrix of the tumor septae and the surrounding connective tissues. Pulmonary metastases could not be detected in UTSCC2; in UTSCC24A, metastases showed a moderate fibronectin expression in the nucleus and in the cytoplasm.

Laminin-5 was not expressed *in vitro* in both UTSCC2 and UTSCC24A cells. Cancer cells of primary tumors of both cell lines were negative, but there was a laminin-5 expression in the ECM and the stroma of the primary tumors. Small pulmonary metastases showed a moderate laminin-5 cytoplasmic expression, while large metastases were negative. Pan-cytokeratin expression in cell pellets showed a high intensity at the margin of cells in UTSCC2 and UTSCC24A cells. A low intensity pan-cytokeratin expression was detected at the cell margin in cancer cells of primary tumors. UTSCC24A cells showed a slightly stronger expression in primary tumors than in cells grown *in vitro*. Pan-cytokeratin positive cells were notably mainly located at the tumor-host interface and not in the middle of the tumor. Pulmonary metastases were not detected. In contrast, vimentin was negative in cells of both cell lines, irrespective of the tissue of origin. ICAM-1 showed a different expression pattern in UTSCC2 and UTSCC24A cells. While ICAM-1 was generally not expressed in UTSCC2 cells, an intensive membrane-bound ICAM-1 expression was noted in UTSCC24A cells grown *in vitro* and *in vivo* as primary tumors. Some pulmonary micrometastatic cells expressed ICAM-1, while others did not. While UTSCC2 cells were generally EpCAM negative, UTSCC24A cells showed a strong membrane-bound expression in all tissues throughout all tumor cells, irrespective of their localization within the primary tumor.

## Discussion

The present study was designed to analyze the expression of transcription factors regulating EMT in human tumor cells derived from different tumor entities grown both *in vitro* and *in vivo* and correlate their expression with each other. All cancer cell lines investigated had been proven to be spontaneously metastatic in previous *in vivo* xenograft experiments. In addition, we aimed to correlate their expression with markers typical for the mesenchymal or epithelial differentiation of tumor cells. We hypothesized that for the expression of some of these marker proteins, a combination of transcription factors may be necessary and/or that these transcription factors might substitute for each other. A study from Peinado *et al.* already showed that expression of one transcription factor alone is not sufficient for an effective operation of EMT (17). If this observation is transferable to our model systems, a combination of different transcription factors should govern metastatic dissemination.

We first investigated whether the expression of one transcription factor dominated in our systems. Indeed, SLUG was strongly expressed in cancer cells of all tumor cell lines investigated both *in vivo* and *in vitro*. In particular, cells which are localized at the tumor-host interface, where EMT mainly occurs, showed the highest expression of SLUG. Furthermore, SLUG expression was mainly observed in the nucleus, indicating that SLUG is present at the site, where it acts as a transcription factor. We could also show that SLUG was additionally localized within the cytoplasm, albeit with lower intensity of the immunoreactivity in nearly all tumor entities. However, this predominantly nuclear distribution of SLUG immunoreactivity argues that SLUG is inducing EMT, which in turn causes aggressiveness and dedifferentiation, as observed particularly in colorectal cancers (Figure 1).

Co-localization of SLUG in the nucleus with other transcription factors causes an enhancement of the repressive function of SLUG (18). Such a co-expression was also noted in some of our tumor cells. UTSCC 2 and 24 A cells grown *in vitro*, as well as ovarian cancer cell lines SKOV3 and OVCAR 3, mostly showed a nuclear staining of TWIST, which was also noted for SLUG expression in these cell lines, and which would imply a collaboration of these two transcription factors in modulating gene expression. SLUG itself binds to E-box motifs and represses E-cadherin transcription. Presumably, this repressive function of SLUG is supported by TWIST, which results in a poor prognosis. Our findings corroborate those of Martin *et al.* who demonstrated the same expression pattern of SLUG and TWIST in breast cancer cell lines generally different from those used in this study (19). However, they also used MDA-MB-231 cells, and we could confirm their expression pattern in our experiments (19). The co-expression of these two transcription factors is not surprising as the long non-coding RNA colorectal neoplasia differentially expressed (CRNDE) regulates the expression of both transcription factors, and its expression is associated with a poor prognosis in many different cancers (20, 21). In contrast, other cell lines, such as HCT116 and HT29, showed only a cytoplasmic TWIST expression pattern *in vitro*, hence they cannot interact with SLUG in the nucleus at the chromosomal level. Either SLUG expression alone is sufficient to induce metastases formation, as shown in brain metastases of various different organs, or other transcription factors not analyzed in this study take over this role (22). S100A4 can not only appear in the nucleus, but also in the cytoplasm of cancer cells (11). We could observe this different distribution pattern, especially in primary tumors of UTSCC24A and ovarian cancer cell lines SKOV3 and OVCAR3 (Figure 4) where S100A4 has both a nuclear and cytoplasmic localization in these cell lines. This expression pattern is reflected in the clinical study of Lo *et al.* (11) who reported that a high expression and more diverse localization of S100A4 (nuclear and intracellular) in HNSCC

is associated with high TNM staging, with a high grade (G2 or G3) and the presence of more lymph node metastases and thus a poor prognosis. Especially in UTSCC24A cells, where a high S100A4 expression was detected in primary tumors, metastases have also been found with almost the same expression level. In contrast, no metastases were found in pulmonary tissue of the low-metastatic UTSCC2 cell line, which showed just a low or moderate cytoplasmic expression of S100A4 in primary tumors. The presence of metastases was shown only by a very sensitive molecular biology technique and not histologically (our own unpublished results). Our experimental finding thus reflects the clinical observations of Lo *et al.* (11). It is known that the MDA-MB-231 human breast cancer cell line is a triple-negative, very aggressive type of cancer and thus a very mesenchymal differentiated tumor (23). According to this observation, a ZEB1 and ZEB2 up-regulation in MDA-MB-231 cells was detected, and in line with this hypothesis, an up-regulation of the mesenchymal marker vimentin was also observed (Figure 2). It is well established that there is a correlation between the expression of ZEB1 and the expression of vimentin, as a down-regulation of ZEB1 causes a decrease in vimentin expression and therefore a less distinctive migration, invasiveness, colony forming and proliferation (24), hence our experimental findings correspond with these data. In contrast to MDA-MB-231 cells, ZEB1 and ZEB2 are to a lower degree expressed in tumors which are more epithelially differentiated, as in colon cancer (HT29 and HCT116) and HNSCC (UTSCC2 and UTSCC24A) cells that show no or very little vimentin expression. Several studies have highlighted the role of proteins of the BM in the induction of EMT (20, 21). In particular, deposition of fibronectin in the ECM can induce an up-regulation of vimentin in cancer cells. This observation implies that fibronectin can induce EMT by increasing the expression of proteins with mesenchymal properties (25). Hence, a direct correlation could exist between the expression of proteins of the BM and the mesenchymal phenotype. Such a correlation was observed in the case of the breast cancer cell line MDA-MB-231 grown *in vivo*, which showed both a high fibronectin deposition and a high vimentin expression. In contrast to vimentin, EpCAM is a cell adhesion molecule that can be used as an epithelial marker of cancer cells. It showed the highest membrane expression in HT29 and HCT116 primary colon cancer cells grown in SCID mice and in primary tumors of UTSCC24A from HNSCC cells, also grown in SCID mice (26). They are both well-differentiated tumor entities and show an epithelial phenotype.

In comparison, lung metastases of UTSCC24A showed a very weak or no expression of EpCAM. The observation that single cell metastases or very small metastatic deposits can be negative for EpCAM expression has already been made in HT29 colon cancer spontaneous metastases into the lungs,

and it was interpreted as a sign of mesenchymal differentiation of these small deposits, as larger ones were again EpCAM positive (27). The same process obviously happens in the UTSCC24A cells with regard to EMT and MET. In this study, we showed that SLUG is the main transcription factor expressed in human metastatic cancer cells transplanted into immunodeficient mice. Its expression always shows a moderate to high level, and it is the only transcription factor and marker that appears in all tumor entities and cell lines *in vitro* and *in vivo*. In addition, our results show that there are always more than one transcription factor co-expressed with SLUG, especially so *in vivo*. Colon cancer shows a simultaneously moderate to high expression of ZEB2 and SLUG, while TWIST is expressed just at a low level.

## Conclusion

MDA-MB-231 cells show a high expression of almost all transcription factors except TWIST, while ovarian cancer cells shows a simultaneous expression of ZEB1 and SLUG. HNSCC shows an overexpression of SLUG, while ZEB1 and ZEB2 were only expressed at a moderate level. As one or more than one of these transcription factors are co-expressed with SLUG, the cooperation of SLUG with one of these other transcription factors should be investigated further for their role in promoting metastasis formation.

## Conflicts of Interest

The Authors declare that there are no conflicts of interest regarding this study.

## Authors' Contributions

JG established and performed the immunohistochemical staining, JG and US evaluated the histology, CS, DW performed the animal experiments from which the material was taken, RP, BW initiated and designed the experiments and provided material and all authors critically read the manuscript.

## Acknowledgements

The Authors thank T. Cöllen, S. Feldhaus, T. Gosau, C. Knies, H. Maar, M. Märker, J. Schröder-Schwarz for skillful technical assistance. The Authors also thank Ms E. Grundy for her linguistic correction of the original manuscript.

## References

- 1 Savagner P, Yamada KM and Thiery JP: The zinc-finger protein Slug causes desmosome dissociation, an initial and necessary step for growth factor-induced epithelial-mesenchymal transition. *J Cell Biol* 137: 1403-1419, 1997. PMID: 9182671. DOI: 10.1083/jcb.137.6.1403

- 2 Tripathi MK, Misra S, Khedkar SV, Hamilton N, Irvin-Wilson C, Sharan C, Sealy L and Chaudhuri G: Regulation of BRCA2 gene expression by the SLUG repressor protein in human breast cells. *J Biol Chem* 280: 17163-17171, 2005. PMID: 15734731. DOI: 10.1074/jbc.M501375200
- 3 Ma L, Teruya-Feldstein J and Weinberg RA: Tumour invasion and metastasis initiated by microRNA-10b in breast cancer. *Nature* 449(7163): 682-688, 2007. PMID: 17898713. DOI: 10.1038/nature06174
- 4 Elloul S, Silins I, Tropé CG, Benschushan A, Davidson B and Reich R: Expression of E-cadherin transcriptional regulators in ovarian carcinoma. *Virchows Arch* 449: 520-528, 2006. PMID: 17024425. DOI: 10.1007/s00428-006-0274-6
- 5 Thiery JP: Epithelial-mesenchymal transitions in tumour progression. *Nat Rev Cancer* 2: 442-454, 2002. PMID: 12189386. DOI: 10.1038/nrc822
- 6 Cano A, Pérez-Moreno MA and Rodrigo I: The transcription factor snail controls epithelial-mesenchymal transitions by repressing E-cadherin expression. *Nat Cell Biol* 2: 76-83, 2000. PMID: 10655586. DOI: 10.1038/35000025
- 7 Bendoraitis A, Knouf EC and Garg KS: Regulation of miR-200 family microRNAs and ZEB transcription factors in ovarian cancer: evidence supporting a mesothelial-to-epithelial transition. *Gynecol Oncol* 116: 117-125, 2010. PMID: 19854497. DOI: 10.1016/j.ygyno.2009.08.009
- 8 Hu X, Macdonald DM and Huettner PC: A miR-200 microRNA cluster as prognostic marker in advanced ovarian cancer. *Gynecol Oncol* 114: 457-464, 2009. PMID: 19501389. DOI: 10.1016/j.ygyno.2009.05.022
- 9 Chu PY, Hu FW and Yu CC: Epithelial-mesenchymal transition transcription factor ZEB1/ZEB2 co-expression predicts poor prognosis and maintains tumor-initiating properties in head and neck cancer. *Oral Oncol* 49: 34-41, 2013. PMID: 22892238. DOI: 10.1016/j.oraloncology.2012.07.012
- 10 Spaderna S, Schmalhofer O and Wahlbuhl M: The Transcriptional repressor ZEB1 promotes metastasis and loss of cell polarity. *Cancer Res* 68: 537-544, 2008. PMID: 18199550. DOI: 10.1158/0008-5472.CAN-07-5682
- 11 Lo JF, Yu CC and Chiou SH: The epithelial-mesenchymal transition mediator S100A4 maintains cancer-initiating cells in head and neck cancers. *Cancer Res* 71: 1912-1923, 2011. PMID: 21169409. DOI: 10.1158/0008-5472.CAN-10-2350
- 12 Thiery JP, Acloque H, Huang RYJ and Nieto MA: Epithelial-mesenchymal transitions in development and disease. *Cell* 139: 871-890, 2009. PMID: 19945376. DOI: 10.1016/j.cell.2009.11.007
- 13 Lenander C, Roblick UJ and Habermann JK: Laminin 5 c 2 chain expression: a marker of early invasiveness in colorectal adenomas. *Mol Pathol* 56: 342-346, 2003. PMID: 14645697. DOI: 10.1136/mp.56.6.342
- 14 Schumacher U and Adam E: Lectin histochemical HPA-binding pattern of human breast and colon cancers is associated with metastases formation in severe combined immunodeficient mice. *Histochem J* 29: 677-684, 1997. PMID: 9413741. DOI: 10.1023/A:1026404832394
- 15 Dippel V, Milde-Langosch K and Wicklein D: Influence of L1-CAM expression of breast cancer cells on adhesion to endothelial cells. *J Cancer Res Clin Oncol* 139: 107-121, 2013. PMID: 22983139. DOI: 10.1007/s00432-012-1306-z
- 16 Oliveira-Ferrer L, Rößler K and Haustein V: c-FOS suppresses ovarian cancer progression by changing adhesion. *Br J Cancer* 110: 753-763, 2014. PMID: 24322891. DOI: 10.1038/bjc.2013.774
- 17 Peinado H, Olmeda D and Cano A: Snail, Zeb and bHLH factors in tumour progression: an alliance against the epithelial phenotype? *Nat Rev Cancer* 7: 415-428, 2007. PMID: 17508028. DOI: 10.1038/nrc2131
- 18 Singh S and Gramolini AO: Characterization of sequences in human TWIST required for nuclear localization. *BMC Cell Biol* 10: 47, 2009. PMID: 19534813. DOI: 10.1186/1471-2121-10-47
- 19 Martin TA, Goyal A, Watkins G and Jiang WG: Expression of the transcription factors snail, slug, and twist and their clinical significance in human breast cancer. *Ann Surg Oncol* 12: 488-496, 2005. PMID: 15864483. DOI: 10.1245/ASO.2005.04.010
- 20 Wang W, Yuan F and Xu J: The prognostic role of long noncoding RNA CRNDE in cancer patients: a systematic review and meta-analysis. *Neoplasma* 66: 73-82, 2019. PMID: 30509091. DOI: 10.4149/neo\_2018\_180320N191
- 21 Zhu L and Yang N: LncRNA CRNDE promotes the epithelial - mesenchymal transition of hepatocellular carcinoma cells *via* enhancing the Wnt/ $\beta$ -catenin signaling pathway. *J Cell Biochem*, 2018. PMID: 30430650. DOI: 10.1002/jcb.26762
- 22 Nagaiishi M, Nakata S, Ono Y, Hirata K, Tanaka Y and Suzuki K: Tumoral and stromal expression of Slug, ZEB1, and ZEB2 in brain metastasis. *J Clin Neurosci* 46: 124-128, 2017. PMID: 28890036. DOI: 10.1016/j.jocn.2017.08.050
- 23 Kao J, Salari K and Bocanegra M: Molecular profiling of breast cancer cell lines defines relevant tumor models and provides a resource for cancer gene discovery. *PLoS One* 4: e6146, 2009. PMID: 19582160. DOI: 10.1371/journal.pone.0006146
- 24 Wang L, Pan S, Chang Y, Hung P and Kao S: MDA-9/Syntenin-Slug transcriptional complex promote epithelial-mesenchymal transition and invasion/metastasis in lung adenocarcinoma. *Oncotarget* 7: 386-401, 2015. PMID: 26561205. DOI: 10.18632/oncotarget.6299
- 25 Park J and Schwarzbauer JE: Mammary epithelial cell interactions with fibronectin stimulate epithelial-mesenchymal transition. *Oncogene* 33: 1649-1657, 2014. PMID: 23624917. DOI: 10.1038/onc.2013.118
- 26 Andratschke M, Hagedorn H and Nerlich A: Expression of the epithelial cell adhesion molecule and cytokeratin 8 in head and neck squamous cell cancer: A comparative study. *Anticancer Res* 35: 3953-3960, 2015. PMID: 26124342.
- 27 Jojović M, Adam E, Zangemeister-Wittke U and Schumacher U: Epithelial glycoprotein-2 expression is subject to regulatory processes in epithelial-mesenchymal transitions during metastases: An investigation of human cancers transplanted into severe combined immunodeficient mice. *Histochem J* 30: 723-729, 1998. PMID: 9873999. DOI: 10.1023/A:1003486630314

Received August 9, 2019

Revised August 30, 2019

Accepted September 9, 2019